

Original Research

Preparation of Multi-Group Magnetic Biochar (MMBC) and Its Mechanism for Adsorption of Pb(II) in Aqueous Solution

Si Wan^{1, 2}, Xiangyu Wang^{1*}, Cuiyu Yuan², Bing Wang^{1, 2}, Huanyu Chen²,
Kun Ouyang², Qiulai Xiang², Deng Zhou³, Runhua Chen^{3**}

¹Faculty of Environmental Science and Engineering, Kunming University of Science and Technology, Kunming 650504, China

²Hunan Research Institute for Nonferrous Metals Co., Ltd., Changsha, China

³College of Environmental Science and Engineering, Central South University of Forestry and Technology, Changsha, China

Received: 19 May 2021

Accepted: 15 November 2021

Abstract

Multi-group magnetic biochar (MMBC) was prepared by encapsulating rice husk biochar (BC) in magnetic nanoiron by the liquid-phase reduction-coprecipitation method. MMBC was characterized, and its adsorption of Pb(II) was investigated. Single-factor influence experiments showed that the efficiency for removal of Pb(II) by MMBC reached 90.85% with a pH of 5.0, an adsorbent addition amount of 1 g•L⁻¹ and a contact time of 2 h. Kinetic analyses showed that pseudo-second-order kinetics express the adsorption process of Pb(II) on MMBC more comprehensively than the pseudo-first-order or Elovich kinetic equations. The adsorption process showed good fitting to the Langmuir, Temkin and Dubinin-Radushkevich (D-R) isotherm models. The maximum saturated adsorption capacity was 66.83 mg•g⁻¹, as calculated by fitting the Langmuir equation (303 K±1). The mechanism for adsorption of Pb(II) involved electrostatic attraction, functional group complexation and ion exchange caused by the surface energy of the material. The rate for removal of Pb(II) by MMBC still reached 65% after five adsorption-desorption and regeneration cycles, which indicated that MMBC was effectively regenerated. Therefore, MMBC is a potential economical and effective remediation agent that can be employed to remove Pb(II) from wastewater.

Keywords: adsorption, biochar, desorption, lead, magnetic functional materials

*e-mail: famdct@sohu.com

**e-mail: chen12@csuft.edu.cn

Introduction

Lead is a toxic heavy metal that is extremely harmful to the human body [1, 2]. Lead cannot be degraded in the natural environment and can be enriched through the food chain. Exposure to lead has been associated with the induction of pathological changes and damage to the central nervous system, digestion system, endocrine system, etc. [3]. At present, effective separation processes for the treatment of divalent cation heavy metal wastewater include chemical precipitation methods, evaporation and solidification methods, electrochemical treatment methods and membrane technology [4, 5]. However, practical application of these processes is often subject to operational difficulties, poor efficiency and economic constraints that make it difficult to adapt the processes to various complex pollution situations. Adsorption is characterized by high efficiency, energy savings, and wide applicability, making this method one of the most popular heavy metal wastewater treatment methods [6, 7]. The most commonly used adsorption materials are resin, graphene, biochar, diatomaceous earth, activated carbon and so on [8-10].

The selection, recycling, secondary utilization and exploration of the adsorption mechanism of adsorption materials have always been the most difficult aspects of adsorption methods. Most adsorption materials are powdery solids, which are easy to disperse in wastewater and thus very difficult to recycle. The high cost and difficult recovery of nano adsorbent limit its wide application [11, 12]. Moreover, saturated adsorption materials contain a large amount of pollutants. If they cannot be recycled shortly after use, secondary pollution can easily occur. The introduction of magnetic nanoiron can effectively solve this problem. Studies have shown that magnetic nanoiron has the characteristics of a large specific surface area, low toxicity, good reactivity, superparamagnetism, etc. It can effectively separate and remove heavy metals in aqueous solution with an external magnetic field. Magnetic nanoiron is widely used in the field of environmental remediation [13-15]. However, as shown by in-depth research findings, due to the influence of van der Waals forces, single particles of magnetic nanoiron are prone to agglomerate in aqueous solution, thereby forming aggregates that result in a significant reduction in specific surface area and adsorption capacity and an increase in cost. If microorganisms or biomass materials can be used as carriers to disperse and stabilize magnetic nanoiron, the capacity for adsorption and removal of Pb(II) will be greatly improved. The preparation of such composite materials can also increase material stability. The prepared materials can be collected by adding a magnetic field. These magnetic properties are beneficial for the recovery of adsorbent materials carrying pollutants and the prevention of secondary pollution.

Rice husk is an extremely common agricultural byproduct. A large amount of rice husk is produced in

agricultural production every year, but its utilization rate is extremely low. Resource utilization should be the first choice for rice husk disposal. In recent years, carbonized rice husk has been used as an adsorbent material to remove various pollutants in wastewater, such as heavy metals and organic pollutants, and has attracted widespread attention [16-18]. Rice husk biochar (BC) has a wide range of sources, low price, nontoxicity and abundant surface-active functional groups [19]. Therefore, it can be used as a good adsorbent material for removing Pb(II) in polluted wastewater. The adsorption and removal of Pb(II) by BC have also been reported. However, BC has problems as an adsorption material, such as an underdeveloped pore structure, an insufficient adsorption and removal capacity, and difficulty in separation and recovery. Therefore, the use of magnetic nanoiron coated on biochar as an adsorbent for heavy metal-contaminated wastewater has been reported [20, 21]. However, there are still problems, such as the unclear adsorption mechanism and potential for desorption-recycling. Therefore, magnetic nanoiron was coated on BC as an adsorbent and used to treat Pb(II) in aqueous solution to further explore the removal mechanism.

The liquid-phase reduction-coprecipitation method was used to coat BC with magnetic nanoiron to prepare MMBC in this study. The prepared MMBC was characterized, and the treatment effect and mechanism for adsorption of Pb(II) in aqueous solution were studied to provide theoretical support and a technical reference for resource utilization of BC and remediation of Pb(II)-polluted wastewater.

Experimental Procedures

Materials

Lead nitrate nonahydrate (analytical grade) was purchased from Sinopharm Chemical Reagent Co., Ltd. (Shanghai, China). The reagents used in the experiment were all analytical reagents.

Synthesis Method of MMBC

The washed rice husk was first pyrolyzed and carbonized at 450°C under anoxic conditions for 3 h, crushed to pass through a 100-mesh sieve, washed with deionized water several times to remove ash and dried at 70°C to obtain BC. As shown in Fig. 1, a small amount of BC was placed in the reaction vessel, and an appropriate amount of $\text{FeSO}_4 \cdot 7\text{H}_2\text{O}$ was added. Then, the reaction vessel was placed on a magnetic stirrer for even mixing.

An appropriate amount of sodium borohydride was accurately weighed and dissolved in deionized water to prepare a strong reducing solution. Then, the stirrer was started with a rotating speed of 200 r/min, and a quantitative feeding device was used to mix

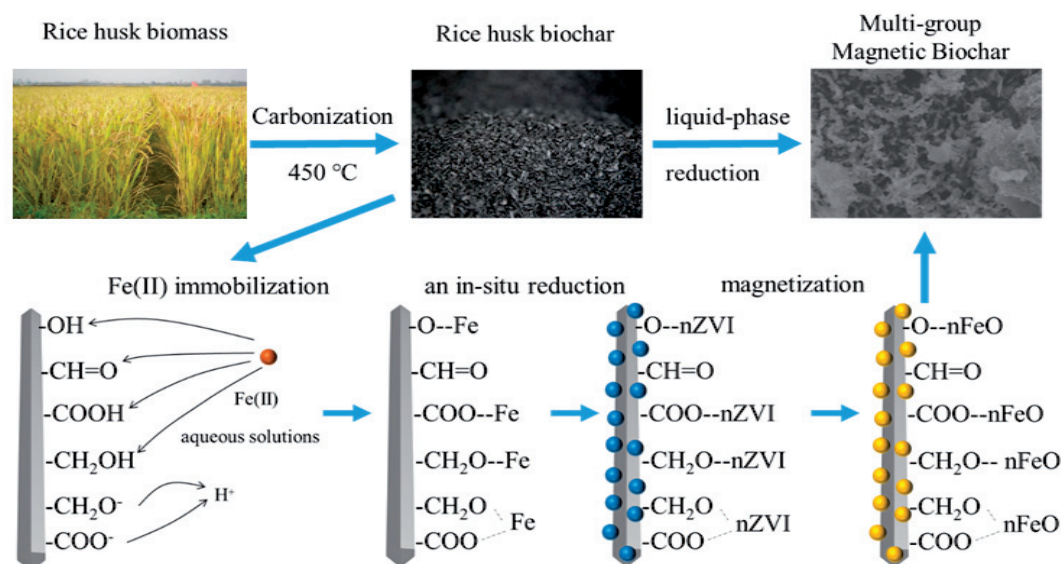


Fig. 1. Preparation of MMBC.

the strong reducing solution into the reaction vessel at a rate of approximately 1 drop per second, thus preparing magnetic BC. The final product was aged for 3 h, washed with absolute ethanol once, washed with deionized water 3 times, oxidized and dried for 24 h in air at 353 K, and then stored in a sealed bag for later use.

Adsorption Experiments

Adsorption experiments were conducted in Erlenmeyer flasks in a constant-temperature shaking box, and the shaking speed was set at 180 r/min. MMBC (0.1 g) was accurately weighed and added to an Erlenmeyer flask containing simulated wastewater with 100 mL Pb(II) (50 mg·L⁻¹). Dilute nitric acid and sodium hydroxide were used to adjust the pH of the Pb(II) solution to 2.0, 3.0, 4.0, 5.0, 5.5, and 6.0. Then, the Erlenmeyer flask was shaken for 2 h at a constant temperature of 303±1 K. The samples were transferred from the Erlenmeyer flask, filtered with a 0.45 μm membrane, and stored for testing.

Different masses of MMBC were accurately weighed and added to 250 mL Erlenmeyer flasks containing 100 mL of simulated wastewater with 50 mg·L⁻¹ Pb(II) to adjust the MMBC addition amount to 0.5-4 g·L⁻¹. The pH was adjusted to 5.0. Then, each Erlenmeyer flask was shaken for 2 h at a constant temperature of 303±1 K. The samples were transferred from the Erlenmeyer flasks, filtered with a 0.45 μm membrane and stored for testing.

MMBC (0.1 g) was accurately weighed and added to a 250 mL Erlenmeyer flask containing 100 mL of simulated wastewater with Pb(II) at an initial concentration of 50 mg·L⁻¹. The pH was adjusted to 5.0. Then, the Erlenmeyer flask was shaken at a constant temperature of 303±1 K for different time intervals

of 5 min, 10 min, 15 min, 30 min, 1 h, 2 h, 4 h, 8 h, 12 h and 24 h. The samples were transferred from the Erlenmeyer flasks, filtered with a 0.45 μm membrane and stored for testing.

MMBC (0.1 g) was accurately weighed and added to a 250 mL Erlenmeyer flask containing 100 mL of simulated wastewater with Pb(II) at an initial concentration of 20-200 mg·L⁻¹. The pH was adjusted to 5.0. Then, the Erlenmeyer flask was shaken at different temperatures of 293±1 K, 303±1 K, 313±1 K and 323±1 K for 2 h. The samples were transferred from the Erlenmeyer flasks, filtered with a 0.45 μm membrane and stored for testing. Three parallel samples were set for all treatments, and the results are given as average values.

Regeneration Cycle Experiments

After reaching adsorption saturation, the MMBC was collected, washed with deionized water and dried at a temperature of 323 K for use. An appropriate amount of the abovementioned adsorbed MMBC was accurately weighed and added to a 250 mL Erlenmeyer flask containing 150 mL of 1 mol/L dilute nitric acid solution. Then, the Erlenmeyer flask was shaken for 24 h at a constant temperature of 303±1 K for desorption. The desorbed MMBC after neutralization was washed with deionized water and dried for later use; this material was called the regenerated adsorbent.

A total of 0.1 g of regenerated adsorbent was accurately weighed and added to a 250 mL conical flask containing 100 mL of simulated wastewater with Pb(II) at a concentration of 50 mg·L⁻¹. The pH was adjusted to 5.0. Then, the Erlenmeyer flask was shaken for 2 h at a constant temperature of 303±1 K. The sample was transferred from the Erlenmeyer flask, filtered with a 0.45 μm membrane and stored for testing. The above

adsorption-desorption regeneration-adsorption process was repeated 5 times.

Analytical Methods

The MMBC was characterized with Fourier transform infrared spectroscopy (FTIR, Thermo Electro Corp, USA), scanning electron microscopy (SEM, Sirion 200, FEI company, USA), Raman spectroscopy (Renish in Via, England), automatic nitrogen adsorption specific surface area analysis (3H-2000BET-A, Beijing), and hysteresis loop measurements (MPMS XL-7, Quantum Design, USA). The lead and copper contents were determined by atomic absorption spectrometry (AAS).

Adsorption Kinetics and Isotherm

The pseudo-first-order model, pseudo-second-order model, Elovich kinetic equation and contact duration (TC) model (303 K) were used to fit the experimental data [22].

Pseudo-first-order kinetic equation

$$q_t = q_e(1 - e^{-k_1 t}) \quad (1)$$

Pseudo-second-order kinetic equation

$$q_t = k_2 q_e^2 t / (1 + k_2 q_e t) \quad (2)$$

Elovich kinetic equation

$$q_t = (1/\beta) \ln(a\beta) + (1/\beta) \ln(t) \quad (3)$$

TC model equation

$$q_t = q_e [1 - (F_{fast} e^{-k_{fast} t} + F_{slow} e^{-k_{slow} t})] \quad (4)$$

In these formulas, q_t and q_e are the capacity for adsorption of Pb(II) at time t and at the time of adsorption equilibrium, respectively; t is the adsorption time (min); k_1 and k_2 are the pseudo-first-order and pseudo-second-order rate constants, respectively; a is the initial adsorption coefficient; β is the desorption rate constant; F_{fast} and F_{slow} are the proportions of fast and slow adsorption reaction components, respectively; and K_{fast} and K_{slow} are the rate constants of fast and slow reactions, respectively.

Results and Discussion

Characterization of MMBC

Fig. 2(a-c) shows SEM images of BC and MMBC. In contrast to BC, MMBC clearly has a large number of mesopores and micropores. The small white particles are nanoiron oxides, which are attached to the surface and inside of BC, increasing the surface roughness and internal pore structure. Measurement results show that the specific surface areas of BC and MMBC are $1.48 \text{ m}^2 \cdot \text{g}^{-1}$ and $56.34 \text{ m}^2 \cdot \text{g}^{-1}$, respectively, which further proves that MMBC has a greatly increased specific surface area compared with BC. Therefore, the surface structure and pores of MMBC are important characteristics for the adsorption of Pb(II) in wastewater.

The results of FTIR analysis are shown in Fig. 2d). BC has a broad absorption band from 3600 cm^{-1}

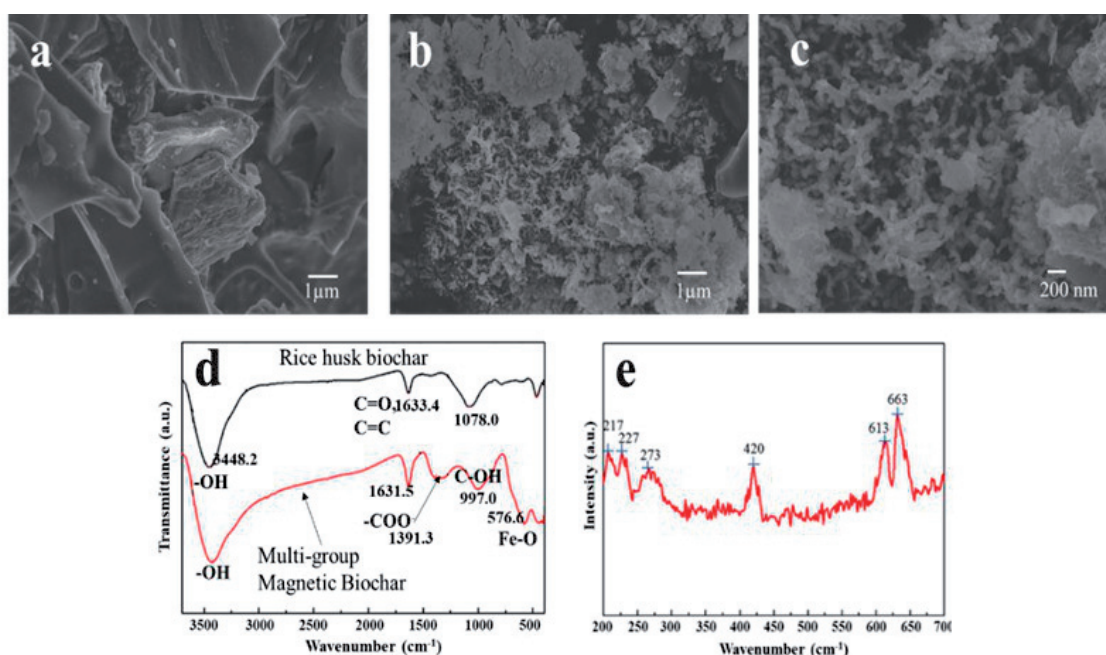


Fig. 2. Characterization of MMBC a), b), c), d), e).

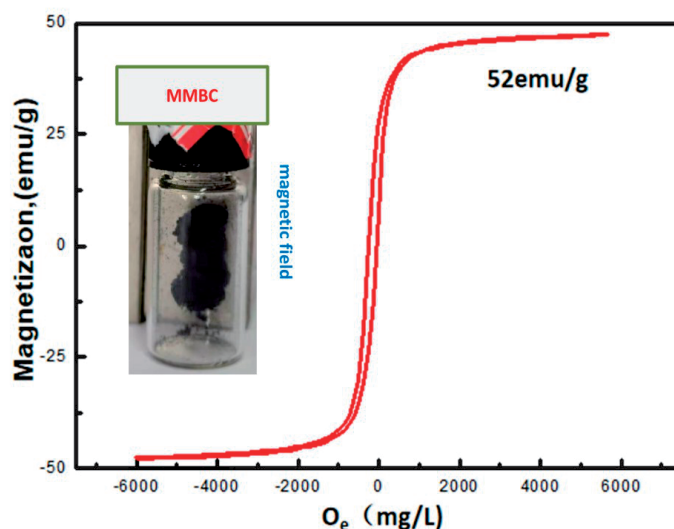


Fig. 3. The Evaluation of Magnetism of MMBC.

to 3200 cm^{-1} , and the maximum absorption peak is located at 3448.2 cm^{-1} , a typical position for a hydroxyl-OH vibration peak. The peak at 1633.4 cm^{-1} is attributed to C=O or aromatic C=C and to C=C/C=O stretching vibrations. The absorption peak at 1078 cm^{-1} may be due to phenolic C-OH stretching vibrations or Si-O. The absorption peak at 470 cm^{-1} corresponds to a Si-O symmetric stretching vibration. SiO₂ and a certain number of functional groups, such as hydroxyl groups and carbon-oxygen double bonds, are evident in the BC structure. The peaks for functional groups corresponding to MMBC are located at 3425 cm^{-1} (-OH hydroxyl stretching vibrations), 1631.5 cm^{-1} (C=O and C=C aromatic vibrations), 1391.3 cm^{-1} (asymmetric and symmetric stretching vibrations of ionic COO⁻), 997 cm^{-1} (C-O stretching) and 576.6 cm^{-1} (Fe-O stretching vibration, the characteristic peak position for Fe₃O₄) [23]. The process for entrapment of magnetic nanoiron caused changes (mostly peak shifts) and increases in the original functional group peaks of BC. After the adsorption of Pb(II), some functional groups of MMBC shifted significantly, such as those at $3425\text{--}3423.1\text{ cm}^{-1}$, $1631.5\text{--}1627.7\text{ cm}^{-1}$, $1391.3\text{--}1384.7\text{ cm}^{-1}$ and $997\text{--}995.1\text{ cm}^{-1}$. The -OH, -C=O, C=C, and -COOH functional groups of the multi-group magnetic biochar participated in the reaction with Pb(II). The mechanism mainly involved complexation with functional groups.

To further clarify the iron valence and composition of the MMBC, Raman spectra in the range 200 cm^{-1} to 700 cm^{-1} were used to analyse the sample, as shown in Fig. 2e). A large amount of nanoiron oxides were present. There were characteristic peaks at 210 cm^{-1} , 227 cm^{-1} , 273 cm^{-1} , 420 cm^{-1} , 613 cm^{-1} and 663 cm^{-1} . By comparison with the peaks of conventional magnetic iron arrays, the peaks at 420 cm^{-1} and 663 cm^{-1} are identified as characteristic peaks of Fe₃O₄ [24], and those at 273 cm^{-1} and 613 cm^{-1} are characteristic peaks of $\alpha\text{-Fe}_2\text{O}_3$. The origins of the peaks at 210 cm^{-1} and 273 cm^{-1} are not yet clear. These peaks are located

close to the characteristic peaks of $\alpha\text{-Fe}_2\text{O}_3$, and it is speculated that the responsible substance may be similar to $\alpha\text{-Fe}_2\text{O}_3$. Therefore, the magnetic properties of multi-group magnetic biochar are derived from nano-Fe₃O₄. The main purpose of encapsulating BC with nanoiron was to enhance the overall adsorption capacity (pre-experimental results, not discussed in the text) and to impart superparamagnetism to the material.

Evaluation of Magnetism

Fig. 3 shows the hysteresis loop of MMBC. Usually, with a hysteresis level of 30–60 emu/g, a material will quickly approach the magnetic field and recover. As shown in Fig. 3, as the magnetic field strength increased, the magnetization of MMBC gradually increased and approached saturation. Its saturation magnetization was 52 emu/g. Therefore, MMBC exhibited fast recovery in a magnetic field, as shown in Fig. 3.

In order to further verify the magnetic separation performance of Fe₃O₄/BC in the actual aqueous solution, a separation test was conducted by a strip magnet with a length of 50mm and a radius of 5 mm. The aqueous solution containing magnetic Fe₃O₄/BC was placed into an Erlenmeyer flask without magnetic field and shaken to a turbid state. Then a bar magnet was moved close to the outer wall of the Erlenmeyer flask. It was found that the turbid solution quickly becomes clear and Fe₃O₄/BC gathers closer to the inner wall of the cone in the direction of the magnet, as shown in the Fig. 3. After removing the magnet and gently shaking the Erlenmeyer flask, the aggregated Fe₃O₄/BC quickly dispersed in the aqueous solution and the solution became mixed again. This verifies the theoretical magnetic separation capability of Fe₃O₄/BC and reveals the recovery performance of Fe₃O₄/BC by magnetic field.

Fig. 4 shows the fitting curve for the kinetics of Pb(II) adsorption on MMBC. The fit parameters are

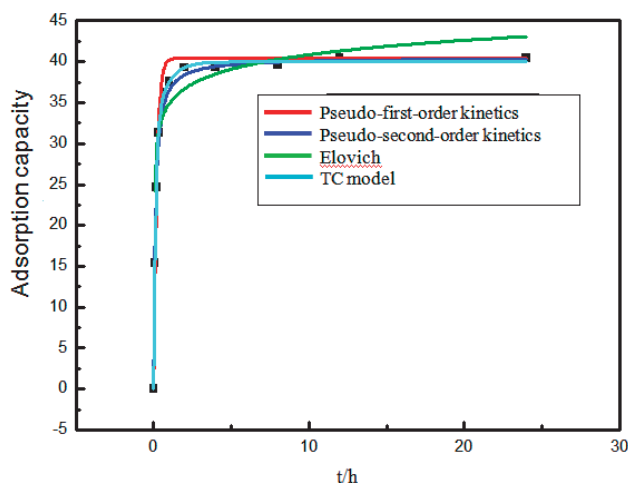


Fig. 4. Fitted adsorption curves for the pseudo-first-order, pseudo-second-order, Elovich, and TC kinetic models.

shown in Table 1. The R^2 for the pseudo-second-order kinetic model was greater than 0.994, indicating that this model described the adsorption process better than the pseudo-first-order or Elovich kinetic models. Generally, pseudo-second-order kinetics are used to describe chemical adsorption via covalent bonding, ion exchange through the sharing of valence bond forces or electron exchange between the adsorbate and adsorbent; these processes comprehensively express the process for adsorption of Pb(II) by MMBC in aqueous solution. Generally, pseudo-second-order kinetics also include membrane diffusion, internal diffusion and surface adsorption. Therefore, the process for adsorption of Pb(II) by multi-group magnetic biochar mainly involves chemical effects. The pseudo-first-order kinetic equation also exhibited a high degree of fit, but this good fit may be due to the initial stage of adsorption and is not suitable for the entire adsorption process. The Elovich kinetic equation is usually used to describe chemical adsorption of highly heterogeneous adsorption materials. In this study, the R^2 value of the Elovich equation reached 0.905, which also indicates that chemical mechanisms play an important role in the adsorption of Pb(II) by MMBC and that the binding sites of MMBC are unevenly distributed.

The TC model divides the adsorption process into two stages: fast and slow. The R^2 value of 0.998 indicated that the process of Pb(II) adsorption by

MMBC was well described by this model. Table 1 shows that the fast adsorption rate (k_{fast}) was much greater than the slow adsorption rate (k_{slow}). Fast adsorption was basically completed in the first 20 min, and the amount adsorbed accounted for 78.21% of the total Pb(II) adsorbed. Then, the system entered the slow adsorption stage. The fast adsorption stage may be due to the functional groups on the MMBC surface, which is consistent with the FTIR analysis results.

The Langmuir equation, Freundlich equation, Temkin equation and Dubinin-Radushkevich (D-R) isotherm adsorption models were used to fit the adsorption of Pb(II) by MMBC in aqueous solution (293-323 K).

Langmuir equation

$$C_e/q_e = 1/(b \cdot q_m) + C_e/q_m \quad (5)$$

Freundlich equation

$$\lg q_e = \lg K_f + 1/n \cdot \lg C_e \quad (6)$$

Temkin equation

$$q_e = RT/b \cdot \ln(a \cdot C_e) \quad (7)$$

D-R equation

$$\begin{aligned} \ln(q_e) &= \ln(q_m) - \beta \varepsilon^2 \\ \varepsilon &= RT \ln(1 + 1/C_e) \\ E_a &= 1/(2\beta)^{1/2} \end{aligned} \quad (8)$$

where C_e is the equilibrium concentration; q_e is the adsorption capacity; q_m is the saturated adsorption capacity; b is a constant related to the adsorption energy; K_f is a constant related to the adsorption affinity; $1/n$ is a constant related to the degree of difficulty of adsorption; a and b are the Temkin constants; RT/b is related to the heat of adsorption ($J \cdot mol^{-1}$); q_m refers to the theoretical maximum adsorption capacity fitted by the D-R equation ($mol \cdot g^{-1}$); E_a is the average adsorption energy ($kJ \cdot mol^{-1}$); β refers to the adsorption free energy ($mol^2 \cdot kJ^{-2}$); and ε is the Polanyi adsorption potential.

The model fitting parameters are shown in Table 2. The Langmuir, Temkin and D-R isotherm models fit the adsorption process well. The R^2 values for the Langmuir model were all greater than or equal to 0.972. This good degree of fit indicated that the adsorption of Pb(II)

Table 1. Kinetic model fitting parameters for Pb(II) adsorption by MMBC.

Pseudo-first-order kinetics			Pseudo-second-order kinetics					
K_1	q_e	R^2	K_2	q_e		R^2		
5.077	40.46	0.984	0.2246	40.53		0.994		
Elovich kinetics			TC model					
a	β	R^2	q_e	F_{fast}	F_{slow}	K_{fast}	K_{slow}	R^2
35.06	-2.524	0.905	39.98	0.7821	0.2179	7.632	1.257	0.998

Table 2. Adsorption isotherm models: related parameters.

T/K	Langmuir Adsorption Model			Freundlich Adsorption Model			
	q_{\max} (mg/g)	K_L	R_L^2	1/n	K_f (L/g)	R_f^2	
293	64.43	0.2645	0.972	0.2658	20.72	0.901	
303	66.83	0.2681	0.972	0.2726	21.12	0.920	
313	69.25	0.2808	0.979	0.2695	22.32	0.916	
323	70.99	0.3423	0.981	0.257	24.41	0.892	
T/K	Temkin Adsorption Model			D-R Adsorption Model			
	A	b	R_T^2	Q_{\max} (mg/g)	β	E_a (kJ·mol ⁻¹)	R_r^2
293	2.36	196.66	0.978	80.79	2.36×10^{-9}	14.55	0.936
303	2.25	186.18	0.976	85.72	2.23×10^{-9}	14.96	0.944
313	2.48	182.42	0.976	88.11	2.06×10^{-9}	15.57	0.943
323	3.07	183.39	0.977	86.91	1.83×10^{-9}	16.53	0.930

on the solid surface of MMBC is a monolayer adsorption process (chemisorption). Theoretically, the adsorption sites on the multi-group magnetic biochar surface are distributed evenly. The maximum adsorption capacity calculated by the Langmuir model (303 K) is 66.83 mg·g⁻¹. q_m gradually rises with increasing temperature, indicating that the adsorption reaction is an endothermic process and that high-temperature conditions are conducive to adsorption. The 1/n parameter value in the Freundlich model was between 0.1 and 1, indicating that the adsorption type belongs to preferential adsorption and that the adsorption performance is high. The K_f value basically increases with increasing temperature, indicating that at higher temperatures, the adsorption affinity of the adsorbate for the adsorbent material is strong. The Temkin model mainly describes a chemical adsorption process based on electrostatic adsorption. The model assumes that the heat of adsorption decreases linearly with a decrease in the degree of coverage of the adsorbent by the adsorbate. In this study, the R^2 of the Temkin model equation fitted to MMBC adsorption of Pb(II) was greater than 0.976. Electrostatic adsorption may be an important mechanism for the interaction between MMBC and Pb(II), which would also verify the effect of pH on the adsorption process.

The D-R isotherm adsorption model is based on Polanyi theory. It does not assume that the adsorbent surface is uniform or that the adsorption potential in the system is constant. This model provides an important basis for distinguishing physical and chemical adsorption. The related literature shows that when E_a has a value of 1-8 kJ·mol⁻¹, physical adsorption is dominant. When E_a has a value of 8-16 kJ·mol⁻¹, the adsorption is based on ion exchange. When E_a has a value of 16-40 kJ·mol⁻¹, the main mechanism is chemical action. In this study, R^2 was greater than 0.930. When the temperature was 293-323 K, E_a reached 14.55 kJ·mol⁻¹,

14.96 kJ·mol⁻¹, 15.57 kJ·mol⁻¹ and 16.53 kJ·mol⁻¹, which means that ion exchange is an important aspect of MMBC adsorption of Pb(II). When the temperature rose, E_a increased, and the chemical effect became more obvious, which is consistent with the Langmuir model fitting results.

Removal of Pb(II) Using MMBC

pH is the key factor affecting adsorption. As shown in Fig. 5a), the pH range in this work was 2.0~6.0. The adsorption capacity of MMBC for Pb(II) was relatively low at lower pH, which may be due to large quantities of H⁺ and Pb(II) competing for active sites. The redox potential of the solution changed with increasing pH, causing the surface-active sites of the MMBC to release lone pairs of electrons and coordinate with Pb(II) empty orbitals, thus increasing adsorption capacity. Considering that a pH higher than 5.5 may lead to hydrolysis of Pb(II), pH = 5.0 was determined to be the best condition for subsequent experiments.

The amount of adsorbent added determines whether the material can provide enough active adsorption sites for Pb(II) adsorption. As shown in Fig. 5b), when the amount of MMBC added was increased from 0.5 g·L⁻¹ to 4.0 g·L⁻¹, the proportion of Pb(II) removed from the simulated wastewater increased sharply from 73.84% to 98.63%. After the amount added exceeded 1 g·L⁻¹, the removal efficiency increased slightly, and it is speculated that adsorption was close to the saturation level. Considering the removal rate, adsorption capacity and economic factors, 1 g·L⁻¹ was determined to be the appropriate addition amount.

The contact time is also an important parameter affecting the adsorption of Pb(II) by MMBC. As shown in Fig. 5c), the process for adsorption of Pb(II) by MMBC in aqueous solution was very fast in the first 20 min and then gradually slowed. After 2 h,

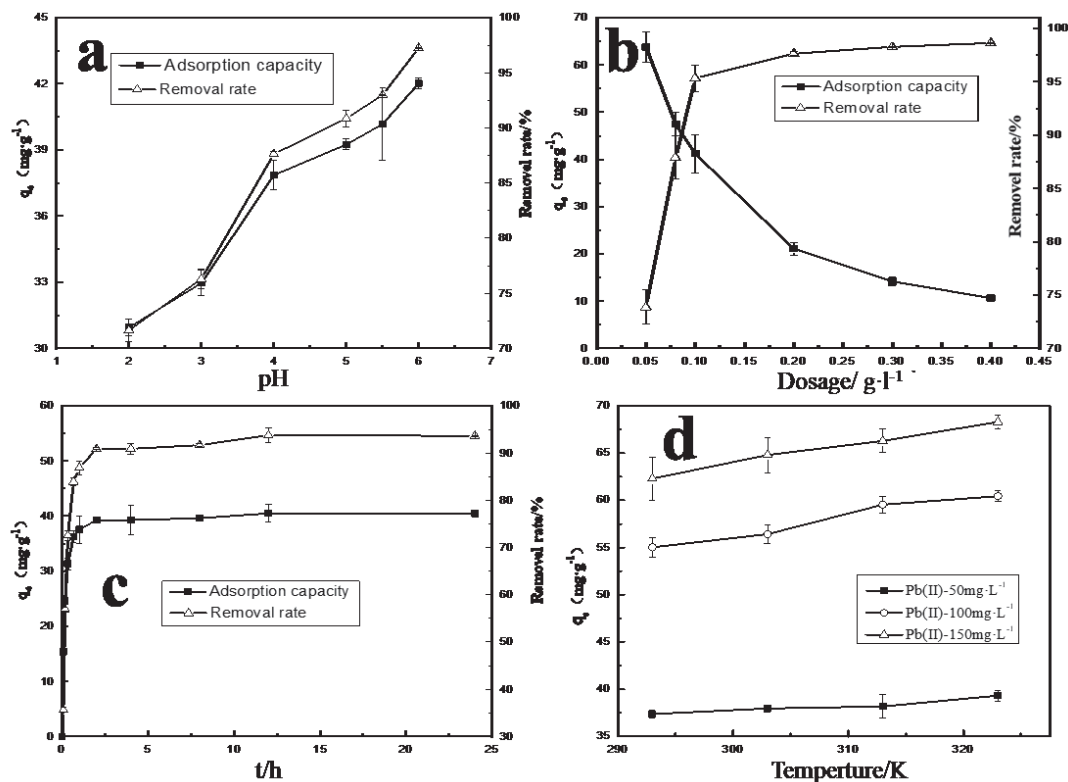


Fig. 5. Effects of different factors on the adsorption of Pb(II) by MMBC: a) pH; b) adsorbent addition amount; c) contact time; d) temperature.

the removal level reached 90.85% and approached a relatively stable state. Therefore, 2 h was the appropriate contact time.

As shown in Fig. 5d), increases in temperature were conducive to the adsorption of Pb(II) and enhanced the removal of Pb(II). When the pH was 5.0 and the Pb(II) concentration was 50 $\text{mg}\cdot\text{L}^{-1}$, 0.1 g of MMBC basically maintained a capacity for adsorption of aqueous Pb(II) of 37-38 $\text{mg}\cdot\text{g}^{-1}$. When the Pb(II) concentration was 100 $\text{mg}\cdot\text{L}^{-1}$, the adsorption capacity increased more obviously with increasing temperature, which may be because chemical adsorption dominated the process for adsorption and removal of Pb(II). Heating increased the activation energy available for chemical reactions and increased the binding capacity of active sites. Therefore, the adsorption capacity increased.

From Fig. 6, the MMBC regeneration cycle experiments showed that the Pb(II) removal efficiency reached 86.2% in the first cycle. After one use and a regeneration cycle, the capacity for Pb(II) adsorption was reduced by nearly 7%, which may be due to structural damage to the MMBC, including the loss of Fe_3O_4 occurring when the original adsorption sites were occupied during the removal of Pb(II) and the regeneration process. After five consecutive adsorption-desorption cycles, the MMBC treatment efficiency still reached 65%. These results show that the MMBC used to treat Pb(II) in aqueous solution has good regeneration capacity and potential for practical application.

Adsorption Mechanism

pH has a significant effect on the removal of Pb(II). Therefore, electrostatic effects on the MMBC surface may be a feature affecting the adsorption of Pb(II). The kinetic results (pseudo-second-order kinetics and Elovich model) showed that chemical adsorption played an important role in the MMBC adsorption of Pb(II). The possible mechanisms for adsorption are

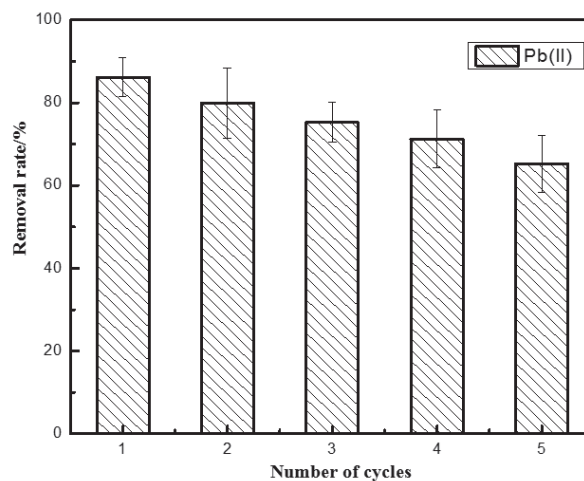


Fig. 6. Study of regeneration cycles for Pb(II) removal by MMBC.

ion exchange and the formation of covalent bonds. The results of isotherm analysis showed that MMBC adsorption of Pb(II) mainly involves electrostatic adsorption (Temkin model), while the D-R adsorption model confirmed that there is an ion exchange mechanism operating in the adsorption process. FTIR analysis showed that functional groups such as -OH, -C=O, C=C, and -COOH participated in the adsorption of Pb(II) via complexation. Various instrumental characterizations of MMBC, including single-factor, kinetic and isothermal thermodynamic analyses, showed that the adsorption of Pb(II) by MMBC in aqueous solution is a complex adsorption process with multiple mechanisms. The adsorption mechanism includes physical and chemical interactions involving electrostatic attraction, functional group complexation, ion exchange and so on.

Conclusions

Magnetic nanoiron was attached to BC to prepare an MMBC composite material, which was used to treat Pb(II) in aqueous solution. After 5 adsorption-desorption cycles, the treatment efficiency of MMBC still reached 65%, indicating that MMBC is a resource-saving and environmentally friendly functional material with recycling capability. The pseudo-second-order kinetic model described the process of MMBC adsorption of Pb(II) well, and the adsorption was divided into two stages: fast adsorption and slow adsorption. The theoretical maximum saturated adsorption capacity obtained by the Langmuir model ($303 \text{ K} \pm 1$, $\text{pH} = 5$) was 66.83 mg/g . The adsorption mechanism of MMBC for Pb(II) involves electrostatic attraction, ion exchange and complexation with surface functional groups on the MMBC.

Acknowledgments

This work was financially supported by the National Key Research and Development Program of China [2019YFC1805201].

Conflict of Interest

The authors declare no conflict of interest.

References

- ROYA B., MOHAMMAD H.M., VADOOD R., HOSSEIN R., SHAHRAM S. Effects of the pre-Cooking process using acetic acid and citric acid on lead concentration in rice. *Pol. J. Environ. Stud.* **29** (1), 545, **2020**.
- SAUSER L., SHOSHAN M.S. Harnessing peptides against lead pollution and poisoning: achievements and prospects. *J. Inorg. Biochem.* **212**, 111251, **2020**.
- MUHAMMAD S., MUHAMMAD Y., MUTI-UR-REHMAN K., AFTAB A.A., MUHAMMAD A., SYED E.H., MUHAMMAD K.R., MUHAMMAD A.I. Assessing lead (Pb) Residues in Lohi Sheep and its impact on hematological and biochemical parameters. *Pol. J. Environ. Stud.* **27** (4), 1717, **2018**.
- CHEN R.H., CHENG Y.Y., WANG P., WANG Q.W., WAN S., HUANG S.H., SU R.K., SONG Y.X., WANG Y.Y. Enhanced removal of Co(II) and Ni(II) from high-salinity aqueous solution using reductive self-assembly of three-dimensional magnetic fungal hyphal/graphene oxide nanofibers. *SCI. TOTAL ENVIRON.* **756**, 143871, **2021**.
- CHEN R.H., CHENG Y.Y., WANG P., WANG Q.W., YAGN Z.H., TANG C.J., XINAG S.Y., LUO S.Y., HUANG S.H., SU C.Q., WANG Y.Y. Facile synthesis of a sandwiched $\text{Ti}_3\text{C}_2\text{T}_x$ MXene/nZVI/fungal hypha nanofiber hybrid membrane for enhanced removal of Be(II) from $\text{Be}(\text{NH}_2)_2$ complexing solutions. *CHEM. ENG. J.* **421**, 129682, **2021**.
- REHMAN M.U., REHMAN W., WASEEM M., HUSSAIN S., HAQ S., REHMAN M.A. Adsorption mechanism of Pb^{2+} ions by Fe_3O_4 , SnO_2 , and TiO_2 nanoparticles. *Environ. Sci. Pollut. Res. Int.* **26** (19), 19968, **2019**.
- XIE Y., YUAN X., WU Z., ZENG G., JIANG L., PENG X., LI H. Adsorption behavior and mechanism of Mg/Fe layered double hydroxide with Fe_3O_4 -carbon spheres on the removal of Pb(II) and Cu(II). *J. Colloid Interface Sci.* **536**, 440, **2019**.
- MOHAMMADI S.Z., MOFIDINASAB N., KARIMI M.A., MOSAZADEH F. Fast and efficient removal of Pb(II) ion and malachite green dye from wastewater by using magnetic activated carbon-cobalt nanoparticles. *Water Sci. Technol.* **82** (5), 829, **2020**.
- XU X.B., HU X., DING Z.H., GAO B. Sorption of aqueous methylene blue, cadmium and lead onto biochars derived from scrap papers. *Pol. J. Environ. Stud.* **29** (6), 4409, **2020**.
- SAIDI S., BOUDRAHEM F., YAHIAOUI I., AISSANI-BENISSAD F. Agar-agar impregnated on porous activated carbon as a new adsorbent for Pb(II) removal. *Water Sci. Technol.* **79** (7), 1316, **2019**.
- WANG Y.Y., ZHENG K.X., ZHAN W.H., HUANG L.Y., LIU Y.D., LI T., YANG Z.H., LIAO Q., CHEN R.H., ZHANG C.S., WANG Z.Z. Highly effective stabilization of Cd and Cu in two different soils and improvement of soil properties by multiple-modified biochar. *Ecotoxicol. Environ. Saf.* **207**, 111294, **2021**.
- WANG Y.Y., LIU Y., WANG Z., NIU L., RUAN X. A field experiment on stabilization of Cd in contaminated soils by surface-modified nano-silica (SMNS) and its phyto-availability to corn and wheat. *J. Soil Sediment.* **20** (1), 91, **2020**.
- CHERAGHIPOUR E., PAKSHIR M. Process optimization and modeling of Pb(II) ions adsorption on chitosan-conjugated magnetite nano-biocomposite using response surface methodology. *Chemosphere.* **260**, 127560, **2020**.
- KLOSTER G.A., VALIENTE M., MARCOVICH N.E., MOSIEWICKI M.A. Adsorption of arsenic onto films based on chitosan and chitosan/nano-iron oxide. *Int. J. Biol. Macromol.* **165** (Pt A), 1286, **2020**.
- LIU Q., MA P., LIU P., LI H., HAN X., LIU L., ZOU W. Green synthesis of stable Fe, Cu oxide nanocomposites from loquat leaf extracts for removal of Norfloxacin and Ciprofloxacin. *Water Sci. Technol.* **81** (4), 694, **2020**.
- HOSSAIN N., NIZAMUDDIN S., GRIFFIN G., SELVAKANNAN P., MUBARAK N.M., MAHLIA T.M.I.

- Synthesis and characterization of rice husk biochar via hydrothermal carbonization for wastewater treatment and biofuel production. *Sci. Rep.* **10** (1), 18851, **2020**.
17. LIU Z., SUN Y., XU X., QU J., QU B. Adsorption of Hg(II) in an aqueous solution by activated carbon prepared from rice husk using KOH activation. *ACS Omega.* **5** (45), 29231, **2020**.
 18. KAMILYA T., MONDAL S., SAHA R. Effect of magnetic field on the removal of copper from aqueous solution using activated carbon derived from rice husk. *Environ. Sci. Pollut. Res. Int.* doi:10.1007/s11356-020-12158-0. **2021**.
 19. SHAMSOLLAHI Z., PARTOVINIA A. Recent advances on pollutants removal by rice husk as a bio-based adsorbent: a critical review. *J. Environ. Manag.* **246**, 314, **2019**.
 20. LIYANAGE A.S., CANADAY S., PITTMAN C.U., JR., MLSNA T. Rapid remediation of pharmaceuticals from wastewater using magnetic Fe₃O₄/Douglas fir biochar adsorbents. *Chemosphere.* **258**, 127336, **2020**.
 21. ZHAO B., XU X., ZHANG R., CUI M. Remediation of Cu(II) and its adsorption mechanism in aqueous system by novel magnetic biochar derived from co-pyrolysis of sewage sludge and biomass. *Environ. Sci. Pollut. Res. Int.* doi:10.1007/s11356-020-11811-y. **2021**.
 22. QU J., TIAN X., JIANG Z., CAO B., AKINDOLIE M.S., HU Q., FENG C., FENG Y., MENG X., ZHANG Y. Multi-component adsorption of Pb(II), Cd(II) and Ni(II) onto microwave-functionalized cellulose: Kinetics, isotherms, thermodynamics, mechanisms and application for electroplating wastewater purification. *J. Hazard. Mater.* **387**, 121718, **2020**.
 23. MENYA E., OLUPOT P.W., STORZ H., LUBWAMA M., KIROS Y., JOHN M.J. Effect of alkaline pretreatment on the thermal behavior and chemical properties of rice husk varieties in relation to activated carbon production. *J. Therm. Anal. Calorim.* **139** (3), 1681, **2020**.
 24. SHEBANOVA O.N., LAZOR P. Raman study of magnetite (Fe₃O₄): laser-induced thermal effects and oxidation. *J. Raman Spectrosc.* **34** (11), 845, **2003**.